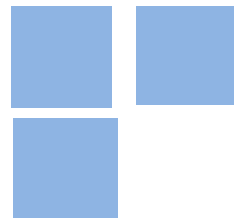


# The Impacts of Palm Oil Expansion on Deforestation and Economic Activity in the Eastern Amazon

**Pedro Henrique B. de Barros**

**Ariaster B. Chimeli**



## **The Impacts of Palm Oil Expansion on Deforestation and Economic Activity in the Eastern Amazon**

Pedro Henrique Batista de Barros (p.batista-de-barros@exeter.ac.uk)

Ariaster Chimeli (chimeli@usp.br)

**Research Group:** [CEMAR; NEREUS]

### **Abstract:**

In recent years, the Brazilian government has designed policies to promote the palm oil industry and forest protection, limiting oil palm plantations to already degraded areas. As a consequence, oil palm crops have increased rapidly in the eastern Amazon region and contributed to a low-carbon energy transition. However, little is known about the effectiveness of these policies in avoiding oil palm-induced deforestation. This paper estimates the impact of oil palm plantations on deforestation and nightlight intensity, a proxy for less land-intensive economic activities that could contribute further to forest protection. We do so in two steps. First, we combined optical spectral bands from Landsat-8 and radar backscatter values from Sentinel-1 to produce a more accurate map of oil palm plantations with a random forest machine learning algorithm. Next, we used the maximum agro-climatically attainable palm oil yield from the Global Agro-Ecological Zoning (GAEZ) as an instrument for oil palm expansion between 2014 and 2020, and estimated the impact of the crop on deforestation and nightlights. Oil palms expanded mainly on pastures, but also contributed to deforestation. We do not find any evidence that the crop stimulates less land-intensive economic activities.

**Keywords:** Oil Palm; Deforestation; Amazon; Remote Sensing.

**JEL Codes:** Q15, Q23, Q28, Q56.

# The Impacts of Palm Oil Expansion on Deforestation and Economic Activity in the Eastern Amazon

Pedro Henrique Batista de Barros\*      Ariaster Baumgratz Chimeli†

## Abstract

In recent years, the Brazilian government has designed policies to promote the palm oil industry and forest protection, limiting oil palm plantations to already degraded areas. As a consequence, oil palm crops have increased rapidly in the eastern Amazon region and contributed to a low-carbon energy transition. However, little is known about the effectiveness of these policies in avoiding oil palm-induced deforestation. This paper estimates the impact of oil palm plantations on deforestation and nightlight intensity, a proxy for less land-intensive economic activities that could contribute further to forest protection. We do so in two steps. First, we combined optical spectral bands from Landsat-8 and radar backscatter values from Sentinel-1 to produce a more accurate map of oil palm plantations with a random forest machine learning algorithm. Next, we used the maximum agro-climatically attainable palm oil yield from the Global Agro-Ecological Zoning (GAEZ) as an instrument for oil palm expansion between 2014 and 2020, and estimated the impact of the crop on deforestation and nightlights. Oil palms expanded mainly on pastures, but also contributed to deforestation. We do not find any evidence that the crop stimulates less land-intensive economic activities.

Keywords: Oil Palm; Deforestation; Amazon; Remote Sensing.

JEL codes: Q15, Q23, Q28, Q56.

---

\*Postdoctoral Research Fellow in the Land, Environment, Economics and Policy Institute (LEEP) at the University of Exeter Business School Xfi Building, Rennes Drive, Exeter, Devon, EX4 4PU, United Kingdom. Email: [p.batista-de-barros@exeter.ac.uk](mailto:p.batista-de-barros@exeter.ac.uk)

†Full Professor in the Department of Economics at the University of São Paulo, Av. Prof. Luciano Gualberto, 908, Butantã, São Paulo, São Paulo State, Brazil. Email: [chimeli@usp.br](mailto:chimeli@usp.br)

# 1 Introduction

1 Palm oil is the most consumed and exported vegetable oil in the world and is used mainly  
2 as food and in biodiesel production (Villela et al. 2014; Chong et al. 2017). The growing world  
3 demand for this commodity reflects a high production potential, a low production cost, and  
4 incentives to replace fossil fuels with biofuels, resulting in a rapid expansion in palm plantations  
5 (Xu et al. 2021).

6 Palm oil production is mainly located in tropical Southeast Asian countries such as Indonesia  
7 and Malaysia. Brazil is the 10th largest producer in the world, with most production and  
8 expressive growth in the cultivated area concentrated in the state of Pará. More specifically, in  
9 the period 2004-2014, Pará increased its cultivation area by more than 200%, reaching 2190  
10 km<sup>2</sup> in extension and a production level of 900,000 tons of palm oil per year. This growth  
11 consolidated the state as the main producer in the country with more than 95% of national  
12 production (Villela et al. 2014; Carvalho et al. 2015; Benami et al. 2018; Nahum, Santos, and  
13 Santos 2020; Almeida, Vieira, and Ferraz 2020). In any case, the cultivated area is still small  
14 compared to the country's productive potential. This fact is mainly due to high production  
15 costs, a learning curve for oil palm cultivation in its early stages, and problems in the sector's  
16 governance model (Englund et al. 2015; Benami et al. 2018; Brandão et al. 2021).

17 Recognizing the strategic importance of palm oil, Brazil has implemented several programs to  
18 encourage its production. These initiatives include the National Program for the Production and  
19 Use of Biodiesel (*Programa Nacional de Produção e Uso do Biodiesel* - PNPB), the Agroecological  
20 Zoning of Palm Oil Cultivation (*Zoneamento Agroecológico da Cultura de Palma de Óleo* - ZAE),  
21 the Sustainable Palm Oil Production Program (*Programa de Produção Sustentável de Óleo*  
22 *de Palma* - PPSP), and the Pronaf Eco Palm Oil program (*Pronaf Eco Dendê*) (Carvalho  
23 et al. 2015; Englund et al. 2015; Lameira, Vieira, and Toledo 2016; Nahum, Santos, and Santos  
24 2020; Brandão et al. 2021). The ZAE, PPSP, and Pronaf Eco Dendê, in particular, aim to  
25 promote oil palm cultivation in degraded areas while preventing crop-driven deforestation.  
26 Despite the economic benefits associated with palm oil expansion, concerns have been raised  
27 about its possible environmental consequences, particularly the illegal clearing of tropical forests  
28 (Koh and Wilcove 2008; Englund et al. 2015; Xu et al. 2021; Brandão et al. 2021).

29 The recent expansion of oil palms in the eastern Amazon has raised significant environmental  
30 concerns due to the existence of highly biodiverse forests in the region, which can be converted  
31 into plantation areas (Carvalho et al. 2015). Although the existing literature indicates that oil  
32 palm cultivation has been replacing forest areas in the Brazilian Amazon (Carvalho et al. 2015;  
33 Lameira, Vieira, and Toledo 2016; Furumo and Aide 2017; Benami et al. 2018; Almeida, Vieira,  
34 and Ferraz 2020), to the best of our knowledge, there are no articles that estimate the causal  
35 contribution of palm oil expansion to the trade-off between economic activity and deforestation  
36 in the region. That is, little is known about whether oil palm is a driver of deforestation or  
37 simply occupies areas that would be deforested anyway. This reflects the fact that the expansion  
38 of crops is normally associated with several economic, political, and social factors that make it  
39 difficult to measure their causal effects on deforestation (Edwards 2018; Kubitzka and Gehrke  
40 2018; Cisneros, Kis-Katos, and Nuryartono 2021), and because spatially disaggregated data  
41 covering the recent expansion of palm oil in Brazil are still scarce.

42 In other words, the identification of the causal effect of palm oil expansion on deforestation  
43 faces two important challenges: data scarcity and the endogeneity problem. To deal with the  
44 first challenge, we follow the pioneering work of Foster and Rosenzweig (2003) and Burgess  
45 et al. (2012) and use both optical spectral bands from Landsat-8 and radar backscatter data  
46 from Sentinel-1 in a 30 x 30 meter spatial resolution mapping process. We then employed  
47 Machine Learning algorithms to analyze satellite images and map oil palm expansion and  
48 deforestation in the Brazilian Eastern Amazon during the 2014-2020 period. A recent dataset

49 on oil palm plantations in Brazil was released by MapBiomass; however, our approach differs by  
50 integrating both optical and radar satellite data in the mapping process (Souza et al. 2020).<sup>1</sup>  
51 Studies such as Chong et al. 2017 and Xu et al. 2021 highlight the superior performance of this  
52 combined approach for oil palm mapping, as optical and radar sensors operate based on different  
53 physical and electromagnetic principles, capturing complementary information. Additionally,  
54 radar signals can penetrate cloud cover, a significant advantage for mapping in tropical regions  
55 where persistent cloudiness is common.

56 Next, we investigate the impact of oil palm on deforestation and the local economy. Because  
57 palm plantations are concentrated in only four large municipalities, our identification strategy  
58 concentrates on an indicator of economic impacts at the pixel level. More specifically, we follow  
59 Henderson, Storeygard, and Weil (2012) and use satellite data from the NASA/NOAA Visible  
60 Infrared Imaging Radiometer Suite (VIIRS) on nighttime lights as a proxy for more urban and  
61 less land-intensive economic activity. We then address the endogeneity problem by exploring  
62 the fact that each pixel differ exogenously in its productive potential for oil palm cultivation.  
63 In particular, we instrumentalize palm oil expansion using the maximum agro-climatically  
64 attainable oil palm yield from the Global Agro-Ecological Zoning (GAEZ) database calculated  
65 by the United Nation’s Food and Agriculture Organization (FAO). Therefore, we compare pixels  
66 that were converted to oil palm with those that were not in order to estimate the causal impact  
67 of the crop on deforestation and local economic activity.

68 This effort is particularly relevant in light of recent developments in deforestation-free supply  
69 chain regulations, such as those introduced by the European Union and the United Kingdom,  
70 which require the implementation of robust and reliable monitoring systems for commodities  
71 such as palm oil. Our approach could be used for due diligence processes, allowing producers and  
72 suppliers to verify and demonstrate that their products are not sourced from deforested areas,  
73 thus ensuring compliance with global sustainability standards and contributing to environmental  
74 conservation efforts (Oliveira et al. 2024).

75 To summarize our results, we used a Random Forest algorithm that produced an overall  
76 classification accuracy of 94.53% and 95.53% for 2014 and 2020, respectively, which is much  
77 superior to the accuracy presented by the oil palm literature for the Amazon. From the land  
78 use and land cover transition analysis, we observed that oil palm cultivation in the region  
79 expanded significantly, increasing from 1,074 km<sup>2</sup> to 1,849 km<sup>2</sup>—an overall growth of 72.16%.  
80 In particular, 156.88 km<sup>2</sup> (20.24%) of this expansion directly replaced vegetation cover pixels.  
81 Our instrumental variable approach then indicated that oil palm plantations indeed expanded  
82 over forested land and their vicinity experienced a reduction in nightlight intensity, our proxy  
83 for more urban and less land-intensive economic activity.

84 Our work belongs to a growing body of economic literature that examines the causal impacts  
85 of palm oil expansion in tropical developing countries<sup>2</sup> and that leverages satellite-based remote  
86 sensing data to map deforestation and economic activity<sup>3</sup> or to analyze broader economic  
87 phenomena.<sup>4</sup> Additionally, this paper engages with the extensive body of research on the  
88 environmental consequences of oil palm expansion worldwide and in Brazil in particular.<sup>5</sup>

89 This paper is structured into six sections, in addition to this introduction. Section 2 provides  
90 background information on palm oil, while Section 3 details the dataset. Sections 4 and 5 outline

---

1. Lameira, Vieira, and Toledo (2016), Furumo and Aide (2017), and Almeida, Vieira, and Ferraz (2020) also contribute to oil palm mapping, but do not use the integrated approach we adopt here.

2. Edwards (2018), Kubitza and Gehrke (2018), Cisneros, Kis-Katos, and Nuryartono (2021), Krishna and Kubitza (2021), Hellmundt, Cisneros, and Kis-Katos (2024), Abman and Lundberg (2024), and Kraus, Heilmayr, and Koch (2024).

3. Foster and Rosenzweig (2003), Burgess et al. (2012), and Henderson, Storeygard, and Weil (2012).

4. Donaldson and Storeygard (2016).

5. See for example Koh and Wilcove (2008). For the Brazilian case, see Villela et al. (2014), Englund et al. (2015), Carvalho et al. (2015), Benami et al. (2018), and Brandão et al. (2021).

91 the methodological approach and present the results, respectively. Finally, Section 6 concludes  
92 with final considerations and policy implications.

## 93 2 Background

94 Originating from Africa, the oil palm is a perennial crop with a life cycle of approximately  
95 25 years, and its trees can grow up to 20 meters in height. Due to these characteristics, it  
96 resembles a forest more than typical agricultural crops. Palm oil is typically cultivated in  
97 monoculture plantations that exhibit distinct and uniform geometric patterns, which facilitates  
98 its identification in satellite imagery. The crop thrives in humid tropical climates with abundant  
99 rainfall, high solar radiation, and temperatures ranging between 24°C and 32°C (Corley and  
100 Tinker 2008).

101 The production of vegetable oil from oil palm has significant potential, mainly due to its  
102 exceptionally high productivity, which can reach up to 368 tons per square kilometer. In  
103 comparison, soy has a much lower productive potential of just 42 tons per square kilometer  
104 (Carvalho et al. 2015; Englund et al. 2015). This high yield, combined with low production  
105 costs, has driven the exponential growth in global demand for palm oil (Xu et al. 2021). In  
106 Brazil, oil palm cultivation began in the 1970s and experienced rapid expansion in the 2000s,  
107 fueled by its growing demand in the food, cosmetics, and biofuel industries (Villela et al. 2014;  
108 Carvalho et al. 2015; Almeida, Vieira, and Ferraz 2020). The crop is particularly well-suited to  
109 the Amazon region, especially Pará, thanks to its favorable soil and climatic conditions, as well  
110 as the availability of suitable areas for further expansion.

111 The growth in palm oil production in Brazil was significantly driven from the 2000s onward  
112 by key government initiatives. These included the establishment of the PNPB in 2004, the ZAE  
113 under Decree No. 7.172/2010, and the PPSP in 2010 (Lameira, Vieira, and Toledo 2016; Nahum,  
114 Santos, and Santos 2020; Brandão et al. 2021). The PNPB, launched in 2004, aimed to increase  
115 biodiesel production, reduce greenhouse gas emissions, and promote regional development. Palm  
116 oil, with its high productivity, presents significant potential to become a key resource for the  
117 expansion of biodiesel production in Brazil (Carvalho et al. 2015; Nahum, Santos, and Santos  
118 2020).

119 The ZAE and PPSP initiatives were established to regulate the expansion of oil palm  
120 cultivation while ensuring its social and environmental sustainability. The ZAE identified  
121 approximately 130,000 km<sup>2</sup> of deforested areas as suitable for cultivation—roughly 300 times  
122 the size of the current planted area. Its primary goals are to promote inclusive and sustainable  
123 regional economic development and to encourage the substitution of renewable energy sources  
124 for fossil fuels. Building on the ZAE framework, the PPSP was launched to further regulate  
125 palm oil expansion by restricting cultivation to degraded and deforested areas cleared before  
126 2008. This approach incentivizes the recovery of degraded land, generating both social and  
127 environmental benefits (Carvalho et al. 2015; Benami et al. 2018; Brandão et al. 2021).

128 Driven by these institutional incentives, a new frontier of oil palm expansion emerged in Pará  
129 from 2010 onward, mainly replacing degraded pastures in the northeast of the state, a region  
130 with some of the most favorable conditions for palm cultivation in Brazil (Almeida, Vieira, and  
131 Ferraz 2020). Between 2010 and 2014, the area under cultivation increased by approximately  
132 200%. However, it is important to note that about 60% of this expansion occurred near forested  
133 areas, raising environmental concerns. This is because the deforestation associated with oil  
134 palm expansion tends to disproportionately impact adjacent forest regions (Benami et al. 2018).

135 We concentrated our analysis in the municipalities of Acará, Moju, Tailândia, and Tomé-Açu,  
136 known as the oil palm pole in Brazil (Figure 1). Together, they cover an area of 23,014.36 km<sup>2</sup>,  
137 of which a significant portion is located in the ZAE. These municipalities are the main producers  
138 of palm oil in Brazil, accounting for approximately 74.1% of the production in Pará and 72.5%

139 of the total palm oil production in the country in 2023 ([Brazilian Institute of Geography](#)  
 140 [and Statistics \(IBGE\) 2025](#)). They are distinguished by their socioeconomic and agricultural  
 141 dynamism, particularly in the Northeastern region of the state.

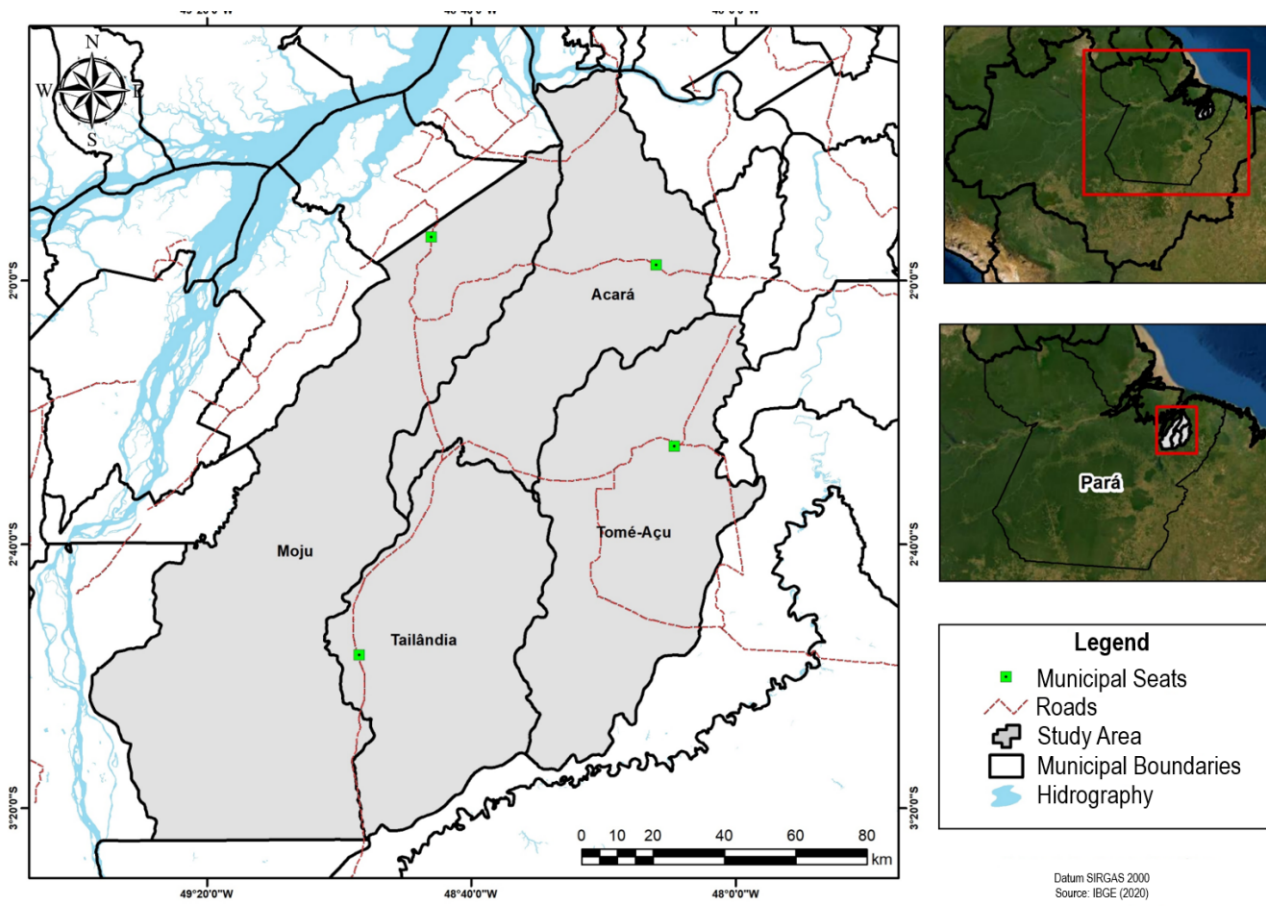


Figure 1: Land use and land cover maps.

142 The region receives an average annual rainfall of 2,500 millimeters, with a minimum monthly  
 143 precipitation of 60 millimeters, which is sufficient to sustain oil palm cultivation without irrigation.  
 144 The terrain is relatively flat, with altitudes ranging from 50 to 100 meters, and an average  
 145 temperature of 26°C. Historically, the landscape was predominantly used for cattle ranching,  
 146 which expanded in the 1960s after the completion of the BR-010 highway (Belém-Brasília).  
 147 Other economically significant agricultural activities include the cultivation of black pepper,  
 148 açai, eucalyptus for timber, cassava, and rice (Almeida, Vieira, and Ferraz 2020).

149 The region is also located near the Belém Endemism Center, an area recognized for its high  
 150 species endemism, severe habitat fragmentation, and susceptibility to fires, making it one of  
 151 the most deforested and ecologically threatened areas in the Amazon (Manhães, Rocha, Souza,  
 152 et al. 2024). Despite still retaining over half of its area covered by forests, ongoing deforestation  
 153 pressures pose significant environmental risks. During our study period, the forest area decreased  
 154 from 13,281.43 km<sup>2</sup> (57.45%) to 12,556.46 km<sup>2</sup> (54.32%), highlighting the increasing threat to  
 155 biodiversity and ecosystem stability (MapBiomias 2025).

### 156 3 Data

157 In order to conduct our analysis, we collect a number of pieces of information on optical  
 158 imagery and radar data, land use, physical characteristics of the territory and potential socio-

159 conomic drivers of land use and oil palm cultivation.

160

### 161 *Remote sensing and physical characteristics of the territory*

162

163 To map oil palm expansion and vegetation formation between 2014 and 2020, we used optical  
164 imagery from Landsat-8 and radar data from Sentinel-1, generating annual composites based on  
165 median values to address potential seasonality effects. Details of the dataset and methodology  
166 are provided in the following section and the Appendix.

167 We obtained elevation data from global satellite-derived Digital Elevation Models (DEMs),  
168 primarily sourced from the Shuttle Radar Topography Mission (SRTM). SRTM employs inter-  
169 ferometric radar technology to map Earth’s topography with high accuracy, offering elevation  
170 data at 90-meter ( 3 arc-seconds) resolutions. From this dataset, we derived a slope raster using  
171 terrain analysis functions, which calculate the rate of elevation change at each pixel, considering  
172 eight neighboring pixels to enhance local topographic representation. The data are expressed in  
173 radians and represent variations in terrain steepness.

174 Precipitation data were retrieved from the WorldClim database, which offers high-resolution  
175 gridded climate data derived from weather station observations, remote sensing, and interpolation  
176 techniques. This dataset provides monthly average precipitation (mm) at a spatial resolution of  
177 10 arc-minutes ( $\approx 18$  km per pixel), which we aggregated into an annual value for the baseline  
178 year 2014.

179 We extract the maximum potential yield of oil palm from FAO-GAEZ under non-irrigated,  
180 low-input, and low-management conditions, reflecting extensive, minimally intensive cultivation  
181 practices. The yield estimates are based on average climatic conditions for the period 1961–1990,  
182 capturing long-term climatic trends that influence palm oil productivity while excluding potential  
183 impacts from recent climate change. This high-resolution (30 arc-seconds, 0.9 km x 0.9 km)  
184 spatial database is a globally recognized resource to assess the potential of agricultural produc-  
185 tivity, integrating agronomic models, climatic conditions, soil properties and land suitability. In  
186 addition to oil palm, we also obtained yield estimates for soybean, maize, rice, and cassava to  
187 control for possible confounders.

188 To standardize the spatial resolution of our dataset to 30 meters, we applied bilinear resam-  
189 pling to all images with coarser resolutions. This interpolation method computes new pixel  
190 values as a weighted average of the four nearest neighboring pixels, ensuring smoother transitions  
191 and preserving spatial continuity in continuous variables. As a result, our final dataset consists  
192 of 39,946 observations (pixels) covering the study area.

193

### 194 *Land use*

195

196 We used data from MapBiomass Collection 9 to examine transitions in oil palm cultivation  
197 and forest area between 2014 and 2020, as well as the baseline pasture cover in 2014, all at a  
198 30-meter pixel resolution. The MapBiomass dataset provides high-resolution annual land-use  
199 and land-cover maps for Brazil, derived from Landsat imagery, serving as a key resource for  
200 monitoring and analyzing land-use dynamics over time (Souza et al. 2020).

201 To check the robustness of our results, we also use the Hansen et al. (2013) dataset, widely  
202 known as the Global Forest Change (GFC) product. It offers high-resolution (30 meters)  
203 information on forest cover dynamics worldwide. This dataset integrates Landsat imagery with  
204 advanced data processing techniques to systematically map forest cover, loss, and gain from  
205 2000 onwards.

206 In this study, we analyzed forest loss between 2014 and 2020, along with the forest cover in  
207 2000, adjusted for net forest change (gain minus loss) between 2000 and 2014, to estimate the  
208 baseline forest cover in 2014.



212 The transport infrastructure variables (roads, waterways and ports) were obtained from the  
213 MapBiomass Project, which processes and publicly provides data from official sources. These  
214 variables represent regional accessibility and can influence oil palm cultivation decisions by  
215 affecting transportation costs and market access. We also used the Urban Shapefile from the  
216 Brazilian Institute of Geography and Statistics (IBGE) to evaluate the impact of urban proximity  
217 on land use decisions.

218 We extracted mill geolocation data from the Universal Mill List (UML), a comprehensive  
219 global database of palm oil mills designed to improve supply chain transparency and support  
220 sustainable sourcing. Developed in collaboration with the World Resources Institute (WRI),  
221 Rainforest Alliance, Proforest, and Daemeter, the UML integrates data from certification bodies,  
222 industry reports, and company disclosures.

223 Data for conservation units and indigenous land are sourced from the Brazilian National  
224 System of Conservation Units (SNUC) and the National Indian Foundation (FUNAI), providing  
225 spatial data on official geographic boundaries.

226 The 2010 population density dataset used in this study is derived from WorldPop, which  
227 provides high-resolution global population maps (1 km<sup>2</sup> resolution). This data set integrates  
228 census data, satellite imagery (for example, Landsat, Sentinel), and machine learning techniques,  
229 offering detailed insights into population distribution patterns.

230 The Nighttime Light (NTL) data were obtained from VIIRS, onboard the Suomi NPP  
231 satellite, launched in 2011 as part of NASA’s Earth observation program. This data set provides  
232 high-resolution measurements of Earth’s nighttime brightness, using artificial illumination as a  
233 proxy for human activity and economic development. It measures absolute radiance in nanowatts  
234 per square centimeter per steradian (nW/cm<sup>2</sup>/sr), capturing the intensity of emitted or reflected  
235 light at night at a 500-meter spatial resolution, including both stable sources (e.g., urban  
236 lighting) and transient sources (e.g., wildfires and gas flares). For this analysis, we computed  
237 changes in VIIRS-derived radiance between 2014 and 2020 to estimate shifts in economic activity  
238 over time.

## 239 4 Methods

### 240 4.1 Mapping and Classification

241 We mapped palm oil plantations in 2014, 2017, and 2020 by integrating optical imagery  
242 from Landsat-8 and radar imagery from Sentinel-1, extracting relevant features for classification  
243 using machine learning algorithms. We chose 2014 as the baseline year, because Sentinel-1 was  
244 launched and became operational only in that year.

245 Since Sentinel-1 offers 10-meter spatial resolution imagery, we resampled it to 30 meters to  
246 match Landsat-8’s resolution and ensure spatial consistency in data processing. The combination  
247 of spectral and backscatter information from these satellite sources provides critical insights into  
248 biophysical properties, such as biomass, vegetation health, and phenological stages, enabling  
249 accurate land-cover classification.

250 We collected training and testing samples using a random sampling approach, resulting in the  
251 following pixel distributions for each class: (i) Vegetal Formation (3,330 pixels), encompassing  
252 primary and secondary forests; (ii) Oil Palm (1,564 pixels); and (iii) Bare Soil (1,300 pixels),  
253 which included exposed soil, cropland, and pasture.

254 For classification, we implemented multiple machine learning algorithms, including K-Nearest  
255 Neighbors (KNN), Artificial Neural Networks (ANN), Decision Trees (DT), Support Vector

256 Machines (SVM), and Random Forests (RF). During the training phase, we identified the  
 257 most relevant variables, validated the models using the test dataset, and then applied the  
 258 best-performing algorithm for classification.

259 In the post-classification phase, we applied a spatial mode filter and performed a manual  
 260 reclassification of palm oil areas to improve the accuracy of the results, using the 2017 map  
 261 to identify and correct inconsistencies in land-use changes. To track palm oil expansion, we  
 262 conducted a pixel-by-pixel land-use transition analysis between 2014 and 2020. A detailed  
 263 description of each methodological step in the classification and mapping process is provided in  
 264 the Appendix.

## 265 4.2 Empirical Strategy for Causal Inference

266 Identifying the causal impacts of palm oil on deforestation and economic activity is difficult  
 267 due to the endogeneity of its expansion. The high potential costs and benefits of investments in oil  
 268 palm plantations make their location often endogenous with regional characteristics. Estimating  
 269 the causal effects of palm oil expansion involves two main challenges: (i) unobservable variables  
 270 that may be correlated with palm oil expansion, economic activity and deforestation; (ii) reverse  
 271 causality, as a higher rate of deforestation and/or economic activity could also encourage the  
 272 expansion of palm oil.

273 This paper explores an exogenous variation, the maximum potential agro-climatically attain-  
 274 able palm oil yield, to instrumentalize its expansion in the Eastern Amazon and thus estimate  
 275 its causal impact on deforestation and economic activity. The instrument is measured as the  
 276 agro-climatically attainable palm oil yield at the pixel level. It is calculated by FAO-GAEZ  
 277 based on agronomic models and provides data on agroclimatic potential yield for different  
 278 crops and levels of input and management at 30 arc-second (0.9 x 0.9 km) resolution. In this  
 279 paper, we use the maximum potential yield of palm oil under non-irrigated, low-input, and  
 280 low-management conditions for an average climate for the period 1981-2010. We selected the  
 281 low-input level as it has been shown in the literature to have the strongest correlation with the  
 282 actual expansion of oil palm plantations (Kubitza and Gehrke 2018).

283 The first-stage in our instrumental variables (IV) estimation procedure is given by the  
 284 following equation:

$$\Delta Oil\_Palm_i = \alpha + \gamma Yield_i + \delta Controls_i + u_i \quad (1)$$

285 where  $\Delta Oil\_Palm_i$  is a binary variable with value 1 when the pixel  $i$  is converted to the oil  
 286 palm class between 2014 and 2020. By concentrating on changes between 2014 and 2020 we  
 287 hope to capture a more consolidated impact of oil palm plantations on forests and economic  
 288 activity over a longer time span, which accommodates for both direct impacts and indirect  
 289 effects via displacement of other activities, for example.  $Yield_i$  is the maximum agro-climatically  
 290 attainable palm oil yield for pixel  $i$ ,  $Controls_i$  represents a vector of pixel-level control variables  
 291 that include physical attributes (altitude, slope, precipitation, latitude, longitude), 2014 baseline  
 292 population density and land use (forest, pasture and night light); maximum attainable yields  
 293 (for soybean, maize, rice and cassava), infrastructure (distance to roads, waterways, ports, urban  
 294 areas, mills) and distance to conservation units and indigenous land; and  $u_i$  is an error term.  
 295 The first stage intuition is that higher potential yields increase the probability of crop expansion.  
 296 given that palm oil firms decide to expand production based on their expected productivity in  
 297 addition to potential profitability (Edwards 2018).

298 Then, we estimate the following two second-stage equations to measure the impacts of oil  
 299 palm expansion,

$$\Delta Deforestation_i = \alpha + \beta \widehat{\Delta Oil\_Palm}_i + \delta Controls_i + \varepsilon_i \quad (2)$$

$$\Delta Nightlight_i = \alpha + \beta \Delta Oil\_Palm_i + \delta Controls_i + \varepsilon_i \quad (3)$$

where  $\Delta Deforestation_i$  is a binary variable that is equal to 1 when pixel  $i$  changes from the vegetation class to any other class between 2014 and 2020;  $\Delta Nightlight_i$  is the change in night lights within a 500 meters radius from pixel  $i$  during the same period;  $\Delta Oil\_Palm_i$  is the instrumentalized variable from the first stage;  $Controls_i$  are the same controls as in the first stage equation; and  $\varepsilon_i$  is the error term.

We first estimate equations (1) and (2) using a logit specification. For nightlights, we estimate (3) with a linear model. However, the distribution of our database is not uniformly distributed with only 11% and 3,36% of the pixels indicating deforestation and palm oil expansion, respectively. Therefore, it may not be reasonable to expect that pixels with a 50% deforestation probability are more sensitive than other pixels to changes in independent variables, as assumed in the logit model. In this context, to further check the robustness of our results, we re-estimated equations (1) – (2) using the more general and flexible Skewed logistic regression approach (scobit) proposed by Nagler 1994, and which includes the logit model as a special case. The scobit model is better suited to outcomes characterized as rare events, such as deforestation and oil palm expansion in this paper (Alix-García and Millimet 2023). For comparison, we also estimate equation (2) using a binary measure of deforestation from Hansen et al. (2013) (logit and scobit in both stages) and a non-binary measure of deforestation that also includes reforestation from MapBiomass (linear model in the second stage).

The crucial identification hypothesis in our context is that the maximum agro-climatically attainable palm oil yield affects deforestation and economic activity only through the oil palm expansion channel. According to Kubitza and Gehrke (2018), the instrument is highly correlated with the expansion of oil palm, as, together with access to land and markets, yield potential is the main determinant of land use patterns. Despite this, there are still some threats to the identification strategy that need to be addressed.

First, other crops have agroclimatic conditions and expansion patterns that may be similar to those for palm oil. Therefore, the instrument may be capturing potential agricultural productivity in general, which would not allow causal interpretations for the estimated effects. For example, an important input for GAEZ palm oil productivity is precipitation, which in addition to affecting the outcome for alternative tropical crops, also impacts deforestation and economic activity (Chomitz and Thomas 2003). Although the instrument is specific for oil palm, it is important to exclude this threat from the identification strategy. Therefore, we control for the potential yields for other competing agricultural activities such as soybean, maize, rice, and cassava in our estimations. We also accounted for whether the pixel was classified as pasture in the baseline by the MapBiomass project, as this classification could increase the likelihood of palm oil expansion due to regulations introduced by the PPSP.

Second, another possible threat to the identification strategy is that the instrument may be capturing general geographic features at the pixel level that may be correlated with deforestation and economic activity. Since our empirical strategy relies on changes in oil palm, deforestation and night lights for the 2014-2020 period, unobserved time-invariant variables at the pixel level such as geographic features are eliminated from the estimated equations. In addition, we include latitude and longitude variables in our equations to control for potential geographically distributed omitted variables.

Finally, it is also plausible that initial differences in infrastructure, economic scale and conservation status could induce different trends in crop expansion, forest loss, and economic activity. Therefore, we control for the distance of pixel  $i$  to the nearest road, waterways, ports, cities, mills, conservation units and indigenous land to capture the availability of infrastructure, access to markets and protected areas.

## 5 Results

### 5.1 Classification

We selected the preferred oil palm mapping result by first comparing each machine learning algorithm using its overall accuracy and Kappa coefficient estimated in the test sample. In addition, we validated all models with the 5-fold cross-validation method for both feature selection and final classification. The results appear in Table A19 in the Appendix and reflect the statistics after applying the recursive feature elimination method. To check whether the algorithms performed well, we considered the overall accuracy and the Kappa coefficient for the years mapped. The weight of the evidence points at the Random Forest (RF) algorithm as the preferred choice.<sup>6</sup> Therefore, we present only the classification results for the RF algorithm due to its better performance and to maintain the consistency of the following analyses. Finally, we calculate the confusion matrices based on our test samples and present the results in Figure 4 in the Appendix.

Next, we calculated the user’s accuracy (UA) and producer’s accuracy (PA)<sup>7</sup> to assess the robustness of our results. UA represents the proportion of correctly classified pixels within a given class relative to all pixels assigned to it, indicating the reliability of the classification. PA evaluates the proportion of reference pixels for a given class that are correctly classified, reflecting how well the classification captures the actual extent of that class. For oil palm, UA and PA values of 0.865 and 0.866 in 2014, and 0.93 and 0.929 in 2020, respectively, demonstrate the effectiveness of the methodology in distinguishing oil palm plantations from other land-use classes and ensuring reliable monitoring of their expansion. Vegetal formations consistently achieved the highest accuracies, with UA and PA exceeding 0.97 across all years, while bare soil presented slightly lower values, with UA and PA reaching 0.917 and 0.913 in 2020.

Our results is in line with the recent literature. Xu et al. (2021) also compared several algorithms and obtained the best classification performance with the RF algorithm. Although Shaharum et al. (2020) obtain a better overall accuracy and Kappa for the SVM, they emphasize that RF dominated SVM when the criterion is delimitation of the oil palm areas – our goal here. Specifically for the Eastern Amazon, Almeida, Vieira, and Ferraz (2020) also performed a classification exercise using RF and obtained an overall accuracy of 88.06% and a Kappa of 0.85, using Landsat images. The superior results we present here may be due to the combination of optical and radar images. Radar images capture additional geometric information, which allows for better discrimination of targets with unique geometric characteristics such as oil palm.

Next, Figure 5 in the Appendix shows the selected features with the recursive feature elimination method for the Random Forest algorithm. In practice, this method selects the best combination of features for the final classification. The relevant characteristics for oil palm mapping differ depending on the year and may reflect different climatic, phenological, and stage of maturation conditions. For 2014, the method selected 12 features: Landsat.4, Landsat.2, EVI, Endmember.2, DVI, Landsat.3, Landsat.1, Entropy, Setinel\_VV, GI and Sentinel\_VH. For 2017, 15 features stand out: EVI, Landsat.2, Landsat.4, Sentinel\_VH—VV, DVI, Endmember\_1, Sentinel\_NDI, Landsat.1, Sentinel\_VH-VV, Sentinel\_VV, Sentinel\_VH, Entropy, GI, Endmember.2

---

6. In 2014, RF was the best-performing algorithm (accuracy of 94.45% and Kappa of 0.0975) followed by the Support Vector Machine (SVM) (accuracy of 94.03% and Kappa of 0.8993). In 2017, on the other hand, K-Nearest Neighbor (KNN) was the best algorithm (Accuracy of 94.61% and Kappa of 0.9088) followed by RF (Accuracy of 94.28% and Kappa of 0.9031). Finally, in 2020, RF was again the best algorithm (Accuracy of 95.53% and Kappa of 0.9239) followed by KNN (Accuracy of 93.87% and Kappa of 0.8956).

7.

$$UA = \frac{\text{Number of correctly classified pixels for a class}}{\text{Total pixels classified as that class}} ; PA = \frac{\text{Number of correctly classified pixels for a class}}{\text{Total reference pixels for that class}}$$

387 and Contrast. Finally, for 2020, 14 features were selected: EVI, Sentinel\_VH—VV, Landsat.2,  
 388 Landsat.3, Sentinel\_NDI, Sentinel\_VH-VV, Landsat.4, Sentinel\_VH, Landsat.1, DVI, GI, End-  
 389 member\_2, Endmember\_1 and Sentinel\_VV<sup>8</sup>. The final classification retained most variables  
 390 across all years, with RFE primarily eliminating certain texture metrics that contributed little  
 391 to accuracy or introduced redundancy.

392 Features related to Landsat-8 reflectance surface information were more important for  
 393 classifying oil palm areas, especially the enhanced vegetation index (EVI). However, Sentinel-1  
 394 features were also important, with the difference and the ratio between VV and VH appearing  
 395 as the most relevant, respectively. The order of importance differs from those obtained by Xu  
 396 et al. (2021), which used Top of Atmospheric (TOA) data from Landsat-8 and Sentinel-1.

## 397 5.2 Land Use and Land Cover Transition

398 Figure 2 presents land use and land cover maps for the study area and years 2014, 2017, and  
 399 2020, classified with the Random Forest algorithm. Visual inspection of the maps suggests that  
 400 oil palm expansion occurred along roads and in both degraded areas (bare soil), as stimulated  
 401 by oil palm policies in the country, and areas covered with vegetation formation. We obtain  
 402 additional insight on the expansion of oil palm by inspecting changes in land classes over time.  
 403 The areas covered by oil palm and bare soil increased faster between 2014 and 2017 and more  
 404 slowly between 2017 and 2020. These changes translated into a faster rate of decrease in  
 405 vegetation formation in the first period and a slower contraction in the second period.<sup>9</sup>

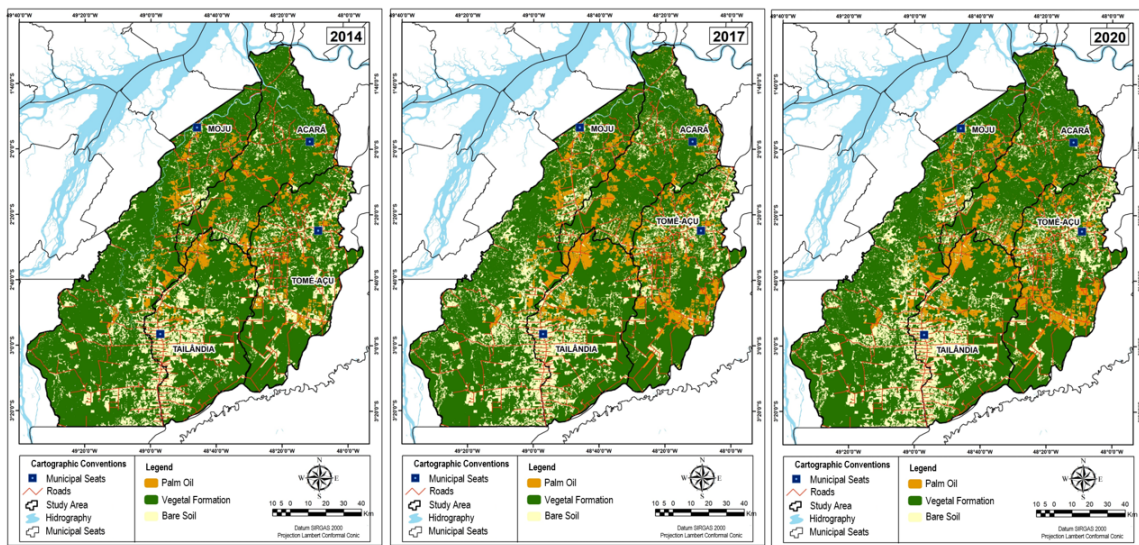


Figure 2: Land use and land cover maps.

406 Comparing our results with those of MapBiomass, they estimated a total of 877.07 km<sup>2</sup> of oil  
 407 palm plantations in 2014, while our study reports an area of 1,074 km<sup>2</sup>. Similarly, MapBiomass  
 408 calculated 1,510.3 km<sup>2</sup> of plantations in 2020, while our study estimates 1,849 km<sup>2</sup> of oil palm

8. The features for 2017 follows the same pattern (Figure 4 in the Appendix), reinforcing the results.

9. The vegetation formation class went from an area of 17,529.57 km<sup>2</sup> (76.37% of the total) in 2014 to 16,436.8 km<sup>2</sup> (71.61%) and in 2017 and 16,289.13 km<sup>2</sup> in 2020 (70.96%). The oil palm class, in turn, had an area of 1,074.93 km<sup>2</sup> (4.68%) in 2014, increasing to 1,703.27 km<sup>2</sup> (7.42%) in 2017 and 1,849.89 km<sup>2</sup> (8.06%) in 2020, an overall growth of 72.16%. Finally, the Bare Soil class had an area of 4,349.72 km<sup>2</sup> (18.95%) in 2014, growing to 4,814.15 km<sup>2</sup> (20.97%) in 2017 and to 4,815.2 km<sup>2</sup> in 2020 (20.98%). The oil palm area expanded over time by 58.45% (2014-2017) and 8.61% (2017-2020), while the bare soil areas increased by 10.68% (2014-2017) and 0.02% (2017-2020). Meanwhile, the area covered by vegetal formation decreased by 6.23% between 2014 and 2017, and by 0.9% between 2017 and 2020. See Figure 6 in the Appendix.

409 farms. This represents an approximate 22.5% increase over the MapBiomias estimate, suggesting  
 410 that the integration of radar imagery with traditional optical data enhances the detection  
 411 and classification of oil palm plantations in the Amazon. In addition, oil palm plantations  
 412 from MapBiomias expanded in both pastures (574.94 km<sup>2</sup>) and natural vegetation (52.52 km<sup>2</sup>)  
 413 between 2014 and 2020. That is, most of the growth occurred within the scope of public policies  
 414 for palm oil in the Brazilian Amazon, but more than 8% of the crop expansion occurred in  
 415 forest areas. Furthermore, pastures occupied an additional 1346.08 km<sup>2</sup> of forest areas during  
 416 the same period, and some of this expansion could be indirectly attributed to oil palm through  
 417 the displacement of consolidated pastures.

418 From the perspective of forests and natural ecosystems, our results indicate that the area  
 419 lost in the vegetation formation class was occupied by both oil palm and bare soil, although the  
 420 latter responded to the lion's share of the cleared land. This, in turn, can be a consequence  
 421 of the fact that the palm oil industry is still relatively small. Therefore, it is important to  
 422 ask whether sustained growth of the palm oil industry is likely to have a significant impact on  
 423 deforestation in the Brazilian Amazon region. To explore this question, we first need to recognize  
 424 that Figure 3 represents an accounting identity for land class changes in the region, but does  
 425 not inform us whether oil palm is indeed a potentially significant driver of local deforestation.  
 426 Our mapping effort is a vital element of the assessment of the impact of the palm oil industry  
 427 on deforestation, but does not clarify whether the deforestation associated with oil palm was  
 428 caused by the crop itself or whether it would have happened anyway due to other socioeconomic  
 429 drivers that cause deforestation (and possibly also the expansion of the palm oil industry). In  
 430 the next section, we present our instrumental variable results for the causal impacts of palm oil  
 431 expansion on deforestation and on an indicator of economic activity. Throughout the analysis,  
 432 we concentrate on land use changes between 2014 and 2020. We chose the longer time frame to  
 433 increase the chance of capturing both direct and indirect impacts of oil palm in forested areas.

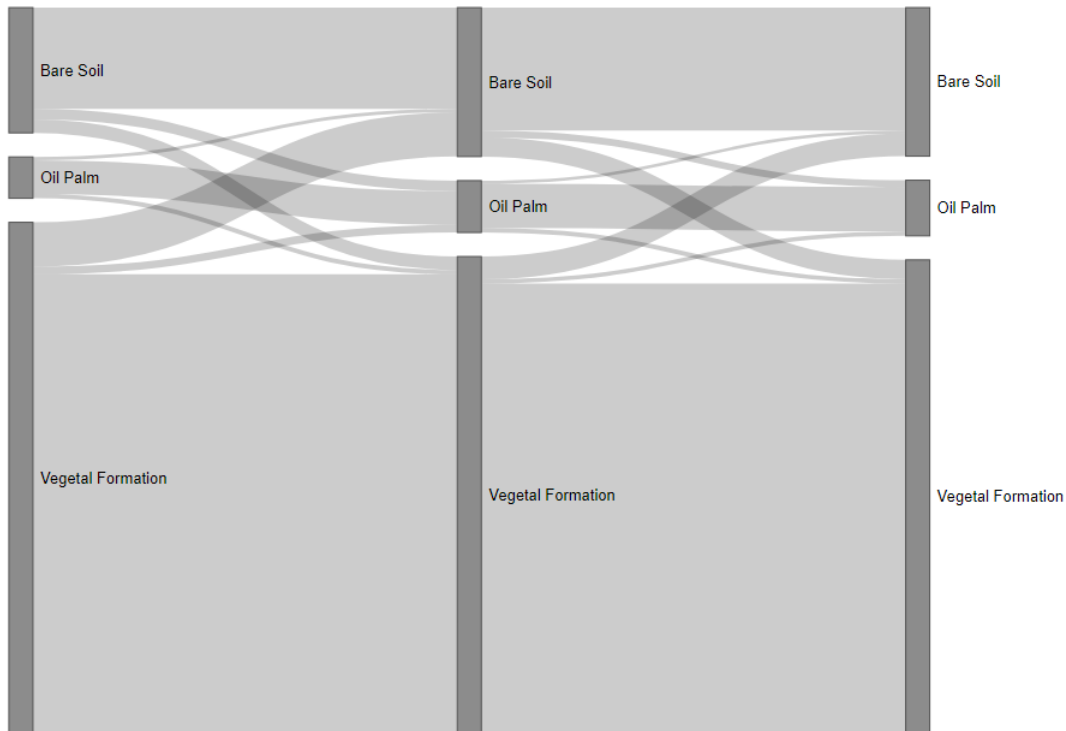


Figure 3: Land use and land cover transitions between 2014-2017 and 2017-2020.

### 5.3 Causal Effects Of Palm Oil Expansion

Table 4 in the appendix reports first-stage estimates from our IV strategy. The oil palm yield potential is positively and significantly correlated with the expansion of oil palm in the region. Furthermore, the size and significance of the yield coefficients are robust to different specifications and the inclusion of a rich set of controls. These results suggest that our instrument does not simply capture broader geographic, agricultural, or socioeconomic determinants of palm oil expansion, thus supporting both the relevance and exclusion restrictions required for the validity of our instrumental variable.

Turning to the main results of interest, Table 1 reports our estimates of oil palm expansion on deforestation (Panel A) and nightlights (Panel B). Column (1) reports naïve correlations that do not account for the endogeneity of oil palm expansion with a logit regression for our binary measure of deforestation and ordinary least squares (OLS) regression for the continuous nightlight variable. In Panel A, both stages rely on either a logit (columns (2) and (3)) or a scobit (columns (4) and (5)) specification, whereas in Panel B, the first stages uses the same strategy as in Panel A, but the second stage relies on a linear regression model.

Although the relationship between oil palm and deforestation is positive and significant in all specifications in Panel A, the estimates in columns (2)–(5) suggest a significant endogeneity bias in the simple correlation estimate from column (1). Adding controls to our models reduces the size of the coefficients, but they remain significant. Panel A suggests that oil palm indeed contributes to deforestation in the region.

In Panel B, the estimated coefficients go from insignificant in column (1) to negative and marginally significant in the IV specifications with controls (p-value of 0.058 in column (3) and 0.068 in column (5)). A sizable and significant increase in light intensity near oil palm plantations could suggest higher returns to complementary activities that are more urban and less land-intensive, which could make investments in deforestation less attractive (Hanusch 2023). However, this does not appear to be the case, at least in the vicinity of the area recently occupied by oil palm. Because our results stem from relatively high spatial resolution data (up to 500 m from a pixel converted to oil palm), they need to be interpreted with caution. For example, Ferreira et al. (2023) use a different methodological approach to examine more aggregated municipal data for a longer period of time (2002-2017) and identify positive spillover effects of oil palm expansion on broader economic activity in the same region.

One potential concern is that our deforestation proxy may not exclusively capture forest clearings, but could also include other land use changes misclassified as vegetation formation. This could put an additional burden of proof on the causal interpretation of our results. To further assess the robustness of our findings, we re-estimate the specifications in Figure 1, Panel A, using the Hansen et al. (2013) dataset. The magnitudes of the coefficients are not directly comparable because Hansen et al. (2013) specifically tracks primary forest loss, whereas we account for both primary and secondary forest loss, as well as degradation of other natural ecosystems. The results align with our main findings, providing further evidence that oil palm expansion is contributing to deforestation in the eastern Amazon.

## 6 Conclusion

Palm oil is the most consumed vegetable oil in the world and a potentially important element of a transition to low-carbon energy. At the same time, it has been associated with large-scale deforestation, ecosystem degradation, and loss of biodiversity in tropical forests, especially in Southeast Asia. The strategic importance of palm oil and ecosystem preservation for a cleaner

Table 1: Impact of Oil Palm Expansion on Deforestation and Nightlights

	<b>Logit (1)</b>	<b>Logit-IV (2)</b>	<b>Logit-IV (3)</b>	<b>Scobit-IV (4)</b>	<b>Scobit-IV (5)</b>
<b>Panel A: Deforestation</b>					
Oil Palm Expansion	0.9190*** (0.0035)	21.6495*** (1.6870)	8.0818*** (0.2990)	20.5510*** (1.6018)	8.4074*** (0.5404)
<i>Marginal Effect</i>	0.9190*** (0.0035)	2.1147*** (0.1654)	0.6495*** (0.0233)	2.1318*** (0.1699)	0.6325*** (0.0281)
	<b>OLS (1)</b>	<b>IV (2)</b>	<b>IV (3)</b>	<b>IV (4)</b>	<b>IV (5)</b>
<b>Panel B: Nightlights</b>					
Oil Palm Expansion	-0.0056 (0.0041)	0.8813*** (0.0754)	-0.0412* (0.0217)	0.8782*** (0.0751)	-0.0353* (0.0193)
Geographic	Yes	No	Yes	No	Yes
Yield potential	Yes	No	Yes	No	Yes
Socioeconomic	Yes	No	Yes	No	Yes
Observations	39,497	39,497	39,497	39,497	39,497

*Notes:* Panel A shows results for deforestation, while Panel B focuses on nightlight. Columns (1) to (5) represent different model specifications as described in the table. Standard errors, shown in parentheses, are clustered at the pixel level.

Table 2: Robustness Checks Using Hansen et al. (2013) Dataset

	<b>Logit (1)</b>	<b>Logit-IV (2)</b>	<b>Logit-IV (3)</b>	<b>Scobit-IV (4)</b>	<b>Scobit-IV (5)</b>
<b>Panel A: Hansen</b>					
Oil Palm Expansion	0.5093*** (0.0753)	4.6325*** (1.1728)	0.7319*** (0.2990)	4.2754*** (1.0852)	0.4666** (0.2368)
<i>Marginal Effect</i>	0.0754*** (0.0111)	0.7046*** (0.1783)	0.1085*** (0.0410)	0.7043*** (0.1782)	0.0775** (0.0393)
Geographic	Yes	No	Yes	No	Yes
Yield potential	Yes	No	Yes	No	Yes
Socioeconomic	Yes	No	Yes	No	Yes
Observations	39,497	39,497	39,497	39,497	39,497

*Notes:* Panel A shows results for deforestation from Hansen et al. (2013), while Panel B focuses on X. Columns (1) to (5) represent different model specifications as described in the table. Standard errors, shown in parentheses, are clustered at the pixel level.



481 economy has led the Brazilian government to design policies to promote oil palm plantations on  
482 already degraded lands and without causing deforestation. This is an especially sensitive issue  
483 in the Brazilian Amazon, where development opportunities for the local population are much  
484 needed and biodiversity along with ecosystem services can hold an important key to a modern  
485 economy.

486 As a consequence of national palm oil policies, the eastern Amazon region has consolidated  
487 itself as the main and fastest growing producer of oil palm in Brazil in recent years. This paper  
488 assesses the broader impacts of palm oil promotion in an area concentrating more than 70% of  
489 Brazilian oil palm plantations. More specifically, we investigate the impact of oil palm on local  
490 deforestation and economic activity. To do so, we tackled two challenges for policy evaluation  
491 in this specific context: the scarcity of high-quality data on the location of oil palm plantations;  
492 and endogeneity bias likely to plague the estimation of causal effects of oil palm on deforestation  
493 and the economy. We address the data scarcity problem by integrating optical imagery from  
494 Landsat-8 and radar imagery from Sentinel-1 in machine learning models to produce a more  
495 accurate map for oil palm plantations. The accuracy of palm oil classification reached 94.53%  
496 in 2014 and 95.53% in 2020, with Kappa coefficients of 0.9075 and 0.9239, respectively. These  
497 results surpass those of similar studies that mapped oil palms in the eastern Amazon without  
498 integrating optical and radar data. Our results indicate that most of the oil palms planted  
499 between 2014 and 2020 occurred in already occupied area and therefore within the scope of  
500 national policies. However, more than 20% of the crop expansion occurred in forest areas. In  
501 addition, we also observed significant deforestation in the region, which could also be indirectly  
502 attributed to oil palm growth through the displacement of consolidated pastures.

503 The land use change figures are nothing more than an accounting identity and our next step  
504 was to estimate the impact of oil palm plantations on local deforestation and nightlights, a  
505 measure of more urban and less land-intensive economic activity. We estimated an instrumental  
506 variable strategy that uses the potential for crop yield as an instrument, and our results suggest  
507 that oil palm contributes indeed to local deforestation. In addition, we do not find any evidence  
508 that it also promotes other less land-intensive activities that could contribute to slowing down  
509 deforestation in the vicinity of the plantations.

510 Although the evidence suggests that policies to promote oil palm plantations in already  
511 degraded areas of the Brazilian Amazon were in great part successful, the fact that a significant  
512 portion of the crop occupies areas previously covered by natural ecosystems and that palm oil  
513 production in the country is still small, but growing, calls for targeted monitoring of oil palm  
514 farms and deforestation in their vicinity. Monitoring the expansion of the palm oil production  
515 chain and enforcement of forest protection at an early stage is strategic both for the industry,  
516 as deforestation might affect their access to international markets, and for the region, which  
517 may benefit from opportunities from the industry and a broader development pattern centered  
518 on the preservation of its natural capital.

## 519 References

- 520 Abman, Ryan, and Clark Lundberg. 2024. “Contracting, market access and deforestation.”  
521 *Journal of Development Economics* 168:103269. <https://doi.org/https://doi.org/10.1016/j.jdeveco.2024.103269>.
- 523 Alix-García, Jennifer, and Daniel L. Millimet. 2023. “Remotely Incorrect? Accounting for Nonclas-  
524 sical Measurement Error in Satellite Data on Deforestation.” *Journal of the Association of*  
525 *Environmental and Resource Economists* 10 (5): 1335–1367. <https://doi.org/10.1086/723723>.

- 526 Almeida, Arlete Silva, Ima Célia Guimarães Vieira, and Silvio F.B. Ferraz. 2020. “Long-term  
527 assessment of oil palm expansion and landscape change in the eastern Brazilian Amazon.”  
528 *Land Use Policy* 90:104321. <https://doi.org/10.1016/j.landusepol.2019.104321>.
- 529 Benami, E, Lisa Curran, M Cochrane, Adriano Venturieri, R Franco, J Kneipp, and A Swartos.  
530 2018. “Oil palm land conversion in Pará, Brazil, from 2006-2014: Evaluating the 2010  
531 Brazilian Sustainable Palm Oil Production Program.” *Environmental Research Letters*  
532 13:034037. <https://doi.org/10.1088/1748-9326/aaa270>.
- 533 Brandão, Frederico, George Schoneveld, Pablo Pacheco, Ima Vieira, Marc Piraux, and Dalva  
534 Mota. 2021. “The challenge of reconciling conservation and development in the tropics:  
535 Lessons from Brazil’s oil palm governance model.” *World Development* 139:105268. <https://doi.org/https://doi.org/10.1016/j.worlddev.2020.105268>.
- 537 Brazilian Institute of Geography and Statistics (IBGE). 2025. *IBGE System for Automatic*  
538 *Retrieval (SIDRA)*. Accessed: February 2025. <https://sidra.ibge.gov.br/home/ipp/brasil>.
- 539 Burger, S. V. 2018. *Introduction to machine learning with R*. 1st edition. p.200. Beijing, [China].
- 540 Burgess, Robin, Matthew Hansen, Benjamin Olken, Peter Potapov, and Stefanie Onder. 2012.  
541 “The Political Economy of Deforestation in the Tropics.” *The Quarterly Journal of Economics*  
542 127:1707–1754. <https://doi.org/10.2307/41812147>.
- 543 Carvalho, Carolina Monteiro de, Semida Silveira, Emilio Lèbre La Rovere, and Allan Yu Iwama.  
544 2015. “Deforested and degraded land available for the expansion of palm oil for biodiesel in  
545 the state of Pará in the Brazilian Amazon.” *Renewable and Sustainable Energy Reviews*  
546 44:867–876.
- 547 Chomitz, Kenneth, and Timothy Thomas. 2003. “Determinants of Land Use in Amazônia: A  
548 Fine-Scale Spatial Analysis.” *American Journal of Agricultural Economics* 85:1016–1028.
- 549 Chong, Khai Loong, Kasturi Devi Kanniah, Christine Pohl, and Kian Pang Tan. 2017. “A  
550 review of remote sensing applications for oil palm studies.” *Geo-spatial Information Science*  
551 20 (2): 184–200. <https://doi.org/10.1080/10095020.2017.1337317>.
- 552 Cisneros, Elías, Krisztina Kis-Katos, and Nunung Nuryartono. 2021. “Palm oil and the politics  
553 of deforestation in Indonesia.” *Journal of Environmental Economics and Management*  
554 108:102453. <https://doi.org/10.1016/j.jeem.2021.102453>.
- 555 Corley, R. H. V., and P. B. H Tinker. 2008. *The Oil Palm*. p.592. John Wiley Sons.
- 556 Donaldson, Dave, and Adam Storeygard. 2016. “The View from Above: Applications of Satellite  
557 Data in Economics.” *Journal of Economic Perspectives* 30 (4): 171–98. <https://doi.org/10.1257/jep.30.4.171>.
- 559 Edwards, Ryan B. 2018. “Export agriculture and regional development: evidence from Indonesia.”
- 560 Englund, Oskar, Göran Berndes, U Martin Persson, and Gerd Sparovek. 2015. “Oil palm for  
561 biodiesel in Brazil—risks and opportunities.” *Environmental Research Letters* 10 (4): 044002.  
562 <https://doi.org/10.1088/1748-9326/10/4/044002>.
- 563 Ferreira, Susane Cristini Gomes, Claudia Azevedo-Ramos, Hilder André Bezerra Farias, and  
564 Pedro Mota. 2023. “Spillover effect of the oil palm boom on the growth of surrounding  
565 towns in the eastern Amazon.” *Land Use Policy* 133:106867. <https://doi.org/https://doi.org/10.1016/j.landusepol.2023.106867>.
- 566

- 567 Foster, Andrew D., and Mark R. Rosenzweig. 2003. "Economic Growth and the Rise of Forests\*." *The Quarterly Journal of Economics* 118 (2): 601–637. [https://doi.org/10.1162/0033553033](https://doi.org/10.1162/003355303321675464)  
568 [21675464](https://doi.org/10.1162/003355303321675464).  
569
- 570 Furumo, Paul, and T. Mitchell Aide. 2017. "Characterizing commercial oil palm expansion in  
571 Latin America: Land use change and trade." *Environmental Research Letters* 12. <https://doi.org/10.1088/1748-9326/aa5892>.  
572
- 573 Gorelick, Noel, Matt Hancher, Mike Dixon, Simon Ilyushchenko, David Thau, and Rebecca  
574 Moore. 2017. "Google Earth Engine: Planetary-scale geospatial analysis for everyone." *Big*  
575 *Remotely Sensed Data: tools, applications and experiences*, *Remote Sensing of Environment*  
576 202:18–27. <https://doi.org/10.1016/j.rse.2017.06.031>.
- 577 Hansen, M. C., P. V. Potapov, R. Moore, M. Hancher, S. A. Turubanova, A. Tyukavina, D.  
578 Thau, et al. 2013. "High-Resolution Global Maps of 21st-Century Forest Cover Change." *Science* 342 (6160): 850–853. <https://doi.org/10.1126/science.1244693>.  
579
- 580 Hanusch, Marek. 2023. *A balancing act for Brazil's Amazonian states: An economic memorandum*.  
581 World Bank Publications.
- 582 Hellmundt, Tobias, Elías Cisneros, and Krisztina Kis-Katos. 2024. "Land-use transformation  
583 and conflict: The effects of oil palm expansion in Indonesia." *SSRN Electronic Journal*  
584 (February). <https://doi.org/10.2139/ssrn.4728074>.
- 585 Henderson, J. Vernon, Adam Storeygard, and David N. Weil. 2012. "Measuring Economic  
586 Growth from Outer Space." *American Economic Review* 102 (2): 994–1028. <https://doi.org/10.1257/aer.102.2.994>.  
587
- 588 Holloway, Jacinta, and Kerrie Mengersen. 2018. "Statistical Machine Learning Methods and  
589 Remote Sensing for Sustainable Development Goals: A Review." *Remote Sensing* 10 (9).  
590 <https://doi.org/10.3390/rs10091365>.
- 591 Kamusoko, C. 2019. *Remote Sensing Image Classification in R*. p.189. Springer Geography.
- 592 Koh, Lian Pin, and David S. Wilcove. 2008. "Is oil palm agriculture really destroying tropical  
593 biodiversity?" *Conservation Letters* 1 (2): 60–64. [https://doi.org/10.1111/j.1755-](https://doi.org/10.1111/j.1755-263X.2008.00011.x)  
594 [263X.2008.00011.x](https://doi.org/10.1111/j.1755-263X.2008.00011.x).
- 595 Kraus, Sebastian, Robert Heilmayr, and Nicolas Koch. 2024. "Spillovers to Manufacturing  
596 Plants from Multimillion Dollar Plantations: Evidence from the Indonesian Palm Oil Boom." *Journal of the Association of Environmental and Resource Economists* 11 (3): 613–656.  
597 <https://doi.org/10.1086/727196>.  
598
- 599 Krishna, Vijesh V., and Christoph Kubitzka. 2021. "Impact of oil palm expansion on the provision  
600 of private and community goods in rural Indonesia." *Ecological Economics* 179:106829.  
601 <https://doi.org/https://doi.org/10.1016/j.ecolecon.2020.106829>.
- 602 Kubitzka, Christoph, and Esther Gehrke. 2018. *Why does a labor-saving technology decrease*  
603 *fertility rates? Evidence from the oil palm boom in Indonesia*. EForTS Discussion Paper  
604 Series 22. University of Goettingen, Collaborative Research Centre 990 "EForTS, Ecological  
605 and Socioeconomic Functions of Tropical Lowland Rainforest Transformation Systems  
606 (Sumatra, Indonesia)".
- 607 Lameira, Wanja Janayna Miranda, Ima Célia Guimarães Vieira, and Peter Mann Mann de  
608 Toledo. 2016. "Expansão da dendeicultura em relação às zonas agroecológicas de Tomé-Açu,  
609 Pará." *Revista Brasileira de Cartografia* 68 (10).

- 610 Liang, Hu, Na Li, and Shengrong Zhao. 2021. “Salt and Pepper Noise Removal Method Based  
611 on a Detail-Aware Filter.” *Symmetry* 13 (3). <https://doi.org/10.3390/sym13030515>.
- 612 Manhães, A.P., F. Rocha, T. Souza, et al. 2024. “Social and biological impact of oil palm (*Elaeis*  
613 *guineensis*) plantations in the Eastern Brazilian Amazon.” *Biodiversity and Conservation*  
614 33:3295–3310. <https://doi.org/10.1007/s10531-024-02913-x>. <https://doi.org/10.1007/s10531-024-02913-x>.
- 616 MapBiomias. 2025. *MapBiomias - Collection of Annual Land Cover and Land Use Maps of Brazil*.  
617 Accessed: February 2025. <https://brasil.mapbiomas.org/en/>.
- 618 Meroni, Michele, Raphaël d’Andrimont, Anton Vrieling, Dominique Fasbender, Guido Lemoine,  
619 Felix Rembold, Lorenzo Seguini, and Astrid Verhegghen. 2021. “Comparing land surface  
620 phenology of major European crops as derived from SAR and multispectral data of  
621 Sentinel-1 and -2.” *Remote Sensing of Environment* 253:112232. <https://doi.org/https://doi.org/10.1016/j.rse.2020.112232>.
- 623 Nagler, Jonathan. 1994. “Scobit: An Alternative Estimator to Logit and Probit.” *American*  
624 *Journal of Political Science* 38 (1): 230–255.
- 625 Nahum, João, Leonardo Santos, and Cleison Santos. 2020. “Formation of palm oil cultivation in  
626 Para’s Amazon.” *Mercator* 19. <https://doi.org/10.4215/rm2020.e19007>.
- 627 Oliveira, Susan E.M., Louise Nakagawa, Gabriela Russo Lopes, Jaqueline C. Visentin, Matheus  
628 Couto, Daniel E. Silva, Francisco d’Albertas, Bruna F. Pavani, Rafael Loyola, and Chris  
629 West. 2024. “The European Union and United Kingdom’s deforestation-free supply chains  
630 regulations: Implications for Brazil.” *Ecological Economics* 217:108053. <https://doi.org/https://doi.org/10.1016/j.ecolecon.2023.108053>.
- 632 Sano, Edson Eyji, Eraldo Aparecido Trondoli Matricardi, and Flávio Fortes Camargo. 2020.  
633 “State-of-the-art of Radar Remote Sensing: Fundamentals, Sensors, Image Processing, and  
634 Applications.” *Revista Brasileira de Cartografia* 72. <https://doi.org/10.14393/rbcv72nespecial50anos-56568>.
- 636 Shaharum, Nur Shafira Nisa, Helmi Zulhaidi Mohd Shafri, Wan Azlina Wan Ab Karim Ghani,  
637 Sheila Samsatli, Mohammed Mustafa Abdulrahman Al-Habshi, and Badronnisa Yusuf.  
638 2020. “Oil palm mapping over Peninsular Malaysia using Google Earth Engine and machine  
639 learning algorithms.” *Remote Sensing Applications: Society and Environment* 17:100287.  
640 <https://doi.org/https://doi.org/10.1016/j.rsase.2020.100287>.
- 641 Somers, Ben, Gregory P. Asner, Laurent Tits, and Pol Coppin. 2011. “Endmember variability in  
642 Spectral Mixture Analysis: A review.” *Remote Sensing of Environment* 115 (7): 1603–1616.  
643 <https://doi.org/10.1016/j.rse.2011.03.003>.
- 644 Souza, Carlos M., Julia Z. Shimbo, Marcos R. Rosa, Leandro L. Parente, Ane A. Alencar,  
645 Bernardo F. T. Rudorff, Heinrich Hasenack, et al. 2020. “Reconstructing Three Decades of  
646 Land Use and Land Cover Changes in Brazilian Biomes with Landsat Archive and Earth  
647 Engine.” *Remote Sensing* 12 (17). <https://doi.org/10.3390/rs12172735>.
- 648 Villela, Alberto A., D’Alembert B. Jaccoud, Luiz P. Rosa, and Marcos V. Freitas. 2014. “Status  
649 and prospects of oil palm in the Brazilian Amazon.” *Biomass and Bioenergy* 67:270–278.  
650 <https://doi.org/10.1016/j.biombioe.2014.05.005>.
- 651 Weiss, M., F. Jacob, and G. Duveiller. 2020. “Remote sensing for agricultural applications: A  
652 meta-review.” *Remote Sensing of Environment* 236:111402. <https://doi.org/10.1016/j.rse.2019.111402>.
- 653

654 Xu, Kaibin, Jing Qian, Zengyun Hu, Zheng Duan, Chaoliang Chen, Jun Liu, Jiayu Sun,  
655 Shujie Wei, and Xiuwei Xing. 2021. “A New Machine Learning Approach in Detecting  
656 the Oil Palm Plantations Using Remote Sensing Data.” *Remote Sensing* 13 (2). <https://doi.org/10.3390/rs13020236>.  
657

## 658 **A Appendix**

### 659 **A.1 Remote Sensing**

660 The increasing availability of satellite images with high spatial, temporal, and spectral  
661 resolution, and in low-cost monitoring techniques, have facilitated their application in economic  
662 and environmental analysis (Donaldson and Storeygard 2016; Weiss, Jacob, and Duveiller  
663 2020). Remote sensing allows you to analyze objects on the Earth’s surface without physical  
664 contact, being basically of two types: active and passive. Passive sensors are normally optical,  
665 capturing the electromagnetic reflectance of targets while active sensors, such as radar and  
666 LIDAR, emit their signals and capture the backscatter effects. Remote sensing data has four  
667 types of resolution: (i) – spatial (pixel size); (ii) – temporal (image frequency); and (iii) –  
668 spectral (electromagnetic spectrum bands); (iv) radiometric (sensitivity).

669 In this paper, we combined optical images from Landsat-8 and radar images from Sentinel-1  
670 from which we extract features to perform the classification. We then collect training and testing  
671 samples, with the most relevant variables selected in the training stage. Finally, we validated  
672 our model on the test sample and used it for classification and mapping.

#### 673 **A.1.1 Images Selection and Composition from Landsat-8 and Sentinel-1**

674 First, we selected Landsat-8 and Sentinel-1 images to compose the database and then mask  
675 the clouds based on the “pixel\_qa” quality band, whose pixel value (322) has no such interference.  
676 Next, we composite the annual images with the median pixels from the collection on the Google  
677 Earth Engine (GEE) platform. Using annual composites and cloud-free images, we integrated  
678 Landsat-8 (30 m) and Sentinel-1 (10 m) data, standardizing the resolution at 30 m to prevent  
679 artificial spatial autocorrelation. The images were pre-processed through GEE’s proprietary  
680 repositories, ensuring suitability for analysis (Gorelick et al. 2017).

#### 681 **A.1.2 Feature Selection and Extraction**

682 From Landsat-8, we used the following spectral bands: (i) – blue; (ii) – green; (iii) – red;  
683 (iv) – infra-red. These spectral information capture important biophysical relationships. For  
684 example, the vegetation biomass is related to the red band - which captures photosynthetic  
685 efficiency - and the near-infrared band - identifies the accumulation of biomass. In this context,  
686 it is common to use vegetation indices that relate the spectral information captured by the  
687 sensors to the health, development, and phenological stages of the vegetation.

688 From Sentinel-1<sup>10</sup> we use the dual-polarized C-band: (i) – VV single co-polarization (vertical  
689 transmit/vertical receive) and (ii) – dual cross polarization VH (vertical transmit/horizontal  
690 receive). Sentinel-1 captures information from the Earth’s surface at a time-frequency of 6 days  
691 considering the equator and at decreasing intervals as it moves towards the poles.

692 Vegetation backscatter values are primarily influenced by leaf angle, size, and water content,  
693 while soil backscatter reflects moisture levels and surface roughness. Additionally, these indices  
694 capture aboveground biomass and the three-dimensional structure of the soil-canopy complex.

---

10. For more information about the state of the art on radar images and their applications, see Sano, Matricardi, and Camargo (2020).

695 Beyond its ability to penetrate cloud cover, Sentinel-1’s Synthetic Aperture Radar (SAR)  
696 provides complementary electromagnetic information, enabling the identification of distinct crop  
697 development characteristics. Consequently, integrating optical and radar sensors significantly  
698 enhances classification accuracy (Meroni et al. 2021).

699 We also generate a linear spectral model of the bare soil fraction and the oil palm fraction  
700 with the Landsat images to reduce the confusion between these two classes, and between oil  
701 palm and forest areas. The spectral mixing model separates the spectral signatures of different  
702 materials contained in a pixel, resulting in components that are called *endmembers*, which in  
703 practice are pure pixels of a target on the earth’s surface (Somers et al. 2011).

704 Next, we calculated vegetation and texture indices for the bands of the Landsat-8 images in  
705 R, using the Rtoolbox and GLCM packages. Vegetation indices are obtained from arithmetic  
706 operations between the different bands of remote sensing images to capture vegetation growth and  
707 structure, as well as soil characteristics and other information related to vegetation development  
708 and health. In particular, we calculated the following vegetation indices: (i) – Difference  
709 Vegetation Index (DVI); (ii) – Ratio Vegetation Index (RVI); (iii) – Greenness Index (GI); (iv)  
710 – Normalized Difference Vegetation Index (EVI); (v) – Enhanced Vegetation Index (EVI); (vi)  
711 – Soil-Adjusted Vegetation Index (SAVI). Among them, it is worth mentioning: (i) – NDVI,  
712 combines information from the red and infrared bands to capture the biomass, however, it  
713 presents saturation from a certain level; (ii) – EVI, combines blue, red, and infrared to correct  
714 atmospheric interference and thus reduce NDVI saturation; (iii) – GCVI, near-infrared and  
715 green to capture chlorophyll concentration to identify nutritional deficit.

716 Finally, we also computed texture indices from the spectral bands of Landsat-8 using the  
717 gray-level co-occurrence matrix (GLCM), which captures key geometric patterns essential for  
718 accurate class discrimination. In particular, we calculated the following characteristics of GLCM  
719 with a 7x7 moving window: (i) – Contrast; (ii) – Angular Second Moment (ASM); (iii) –  
720 Correlation; (iv) – Entropy. According to Xu et al. (2021), these additional information is  
721 essential to improve the classification of oil palm due to its unique geometric characteristics.  
722 We also used Sentinel-1 images to calculate three indicators from the SAR backscattering  
723 values : (i) – ratio (VV/H); (ii) – difference (VV-VH); (iii) normalized difference (NDI) –  
724 (VV-VH)/(VV+VH). The effort resulted in 19 variables that was used to train the classification  
725 algorithms.

### 726 A.1.3 Sampling Process

727 To detect and map oil palm plantations, we collected a training sample of 6,194 observations  
728 through visual interpretation of Landsat-8 images. Samples were categorized into three classes:  
729 Vegetal Formation, Bare Soil, and Oil Palm. Vegetal Formation includes primary forests and  
730 secondary vegetation, while Bare Soil encompasses areas altered by human activity, such as  
731 urban infrastructure, agriculture, pasture and roads.

732 Sampling followed a random selection approach, yielding the following distribution (in pixels):  
733 Vegetal Formation (3,330), Oil Palm (1,564), and Bare Soil (1,300). The dataset was validated  
734 using high-resolution Google Earth imagery. Finally, we randomly split the sample into 80% for  
735 training and 20% for testing to ensure model robustness.

## 736 A.2 Machine Learning

737 The primary goal of Machine Learning<sup>11</sup> is to develop models for prediction or classifica-  
738 tion. Unlike traditional statistical methods, which emphasize asymptotic theory and causal

---

11. See Burger (2018) for a general overview of Machine Learning algorithms, Kamusoko (2019) for remote sensing applications, and Holloway and Mengersen (2018) for agricultural and environmental studies.

739 inference, Machine Learning prioritizes predictive and classification accuracy. There are two  
740 main approaches: supervised and unsupervised learning. In this study, we employed supervised  
741 algorithms to classify remote sensing data, assigning land cover classes to each pixel. To  
742 determine the most effective method, we tested five complementary algorithms: K-Nearest  
743 Neighbors (KNN), Artificial Neural Networks (ANN), Decision Trees (DT), Support Vector  
744 Machines (SVM), and Random Forests (RF).

745 To implement this approach, the model is first trained to minimize misclassification while  
746 avoiding overfitting. This requires splitting the dataset into two subsets: one for training and  
747 another for testing. The testing sample is then used to evaluate the model’s classification  
748 accuracy. To reduce potential bias, we applied sampling techniques, allocating 80% of the data  
749 for training and 20% for testing.

750 To check the robustness of the results, we use a k-fold cross-validation method, with 5-fold,  
751 to ensure that the testing data represents our data sample. This technique splits the data  
752 sample into k chunks and creates, for each chunk, a training and testing sample and estimates  
753 the model. Then, it takes the average of the k predicted errors from each chunk. In other  
754 words, the k-fold cross-validation enables to access the potential classification variation due  
755 to sampling. Next, we adopted the Recursive Feature Elimination (RFE) method, a feature  
756 selection technique that iteratively removes the least important variables to enhance model  
757 performance. RFE trains a model, ranks feature importance, eliminates the weakest predictors,  
758 and repeats this process until the optimal subset is identified. This approach improves accuracy,  
759 reduces dimensionality, and mitigates overfitting.

760 Then, we compare the classification results by applying the trained model to the test sample  
761 to obtain the performance of the estimations in a sample that was not used in the training.  
762 Finally, we compared each classification algorithm based on the classification’s overall accuracy  
763 level and the Kappa coefficient.

### 764 **A.3 Post-classification processing**

765 After classification, we applied a  $7 \times 7$  spatial mode filter to each pixel to reduce the salt-  
766 and-pepper effect, a common issue in pixel-based classifications where isolated misclassified  
767 pixels introduce noise and fragmentation in the image. This effect occurs because pixel-wise  
768 classification ignores spatial dependencies, leading to inconsistencies in neighboring pixels (Liang,  
769 Li, and Zhao 2021). To address this, we used the spatial mode filter from the *raster* package in  
770 R, which assigns each pixel the most frequent class within its surrounding window. This process  
771 enhances spatial coherence and improves the overall accuracy of the classification.

772 Then, we performed a manual reclassification of palm oil areas based on visual interpretation,  
773 considering their geometric characteristics, color, texture, and spatial patterns. This step was  
774 necessary to correct residual misclassified pixels within palm oil cultivation areas that were not  
775 fully addressed by the spatial mode filter. The validation and adjustment process was conducted  
776 using high-resolution imagery from Google Earth, allowing for a more detailed comparison  
777 between the classified map and actual land cover. Common misclassifications included small  
778 patches of bare soil or vegetation being labeled as oil palm and vice versa, often due to spectral  
779 similarities or transitional land cover conditions. By refining the classification through expert  
780 visual assessment, we minimized classification noise, improved spatial coherence, and enhanced  
781 the overall accuracy of the final land cover map, ensuring a more precise and reliable delineation  
782 of oil palm plantations.

783 Finally, we identify land use and land cover transitions between our classes at the pixel level  
784 using the *OpenLand* package in R, which quantifies temporal changes in landscape composition.  
785 This method compares categorical land cover maps from different periods, generating transition  
786 matrices that measure the area or percentage of land shifting from one class to another (e.g.,

787 forest to palm oil). By assessing the extent, direction, and patterns of change, this approach  
 788 provides a detailed understanding of land use dynamic.

## 789 A.4 Results

790  
791

Table 3: Machine Learning Algorithm Performance

Overall Accuracy			
Algorithm	2014	2017	2020
K-Nearest Neighbor	92.54%	94.61%	93.87%
Artificial Neural Network	89.84%	83.51%	78.44%
Decision Tree	86.50%	84.34%	86.74%
Support Vector Machine	94.03%	94.20%	93.29%
Random Forest	94.53%	94.28%	95.53%
Kappa Coefficient			
Algorithm	2014	2017	2020
K-Nearest Neighbor	0.8737	0.9088	0.8956
Artificial Neural Network	0.8284	0.7201	0.6313
Decision Tree	0.7678	0.7305	0.7707
Support Vector Machine	0.8993	0.9022	0.8867
Random Forest	0.9075	0.9031	0.9239

Source: Prepared by the authors.

792  
793

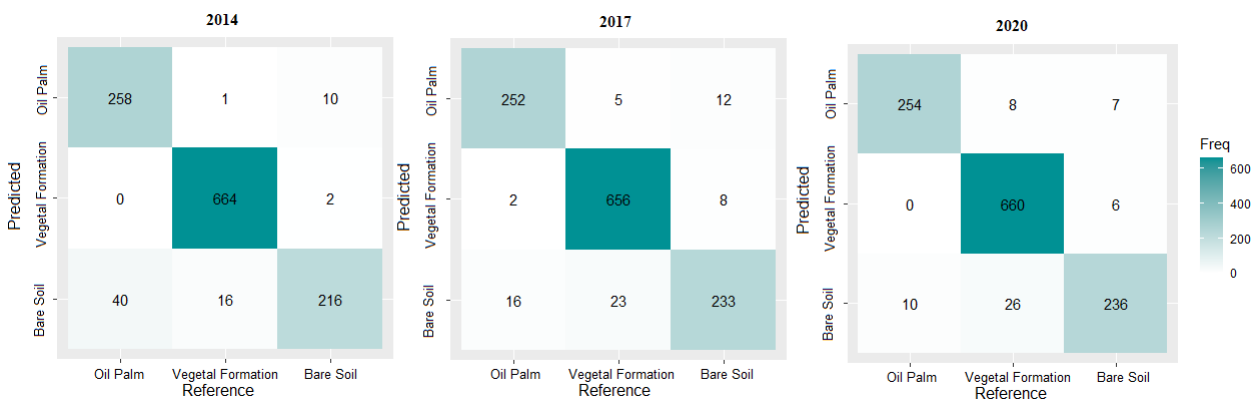


Figure 4: Confusion matrices for the test sample.

794  
795



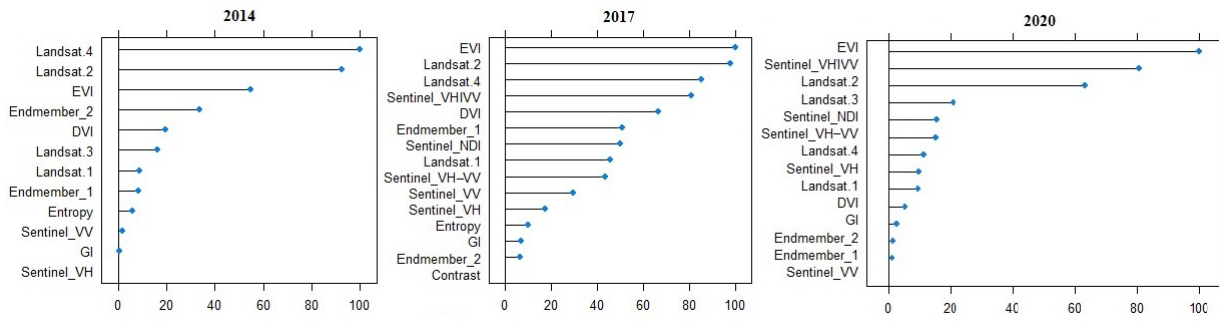


Figure 5: Features – importance for the RF classification.

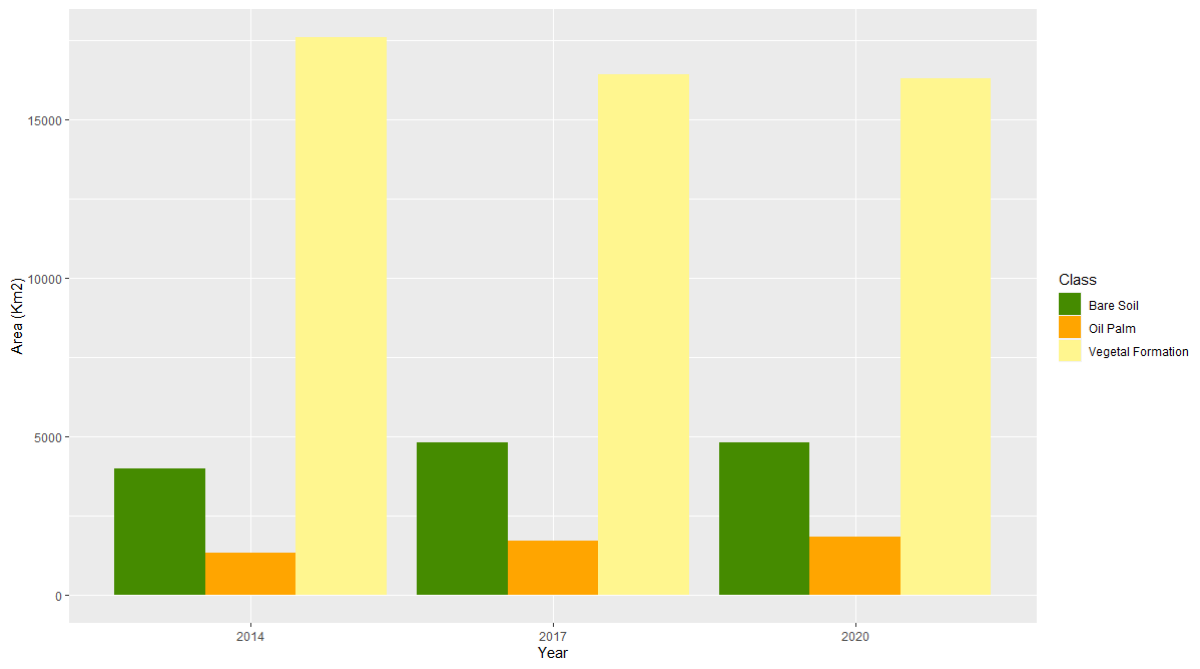


Figure 6: Classes total area in km<sup>2</sup>.

796

797

Table 4: First-Stage Results: Predicting Palm Oil Expansion

	<b>Logit (1)</b>	<b>Logit (2)</b>	<b>Scobit (3)</b>	<b>Scobit (4)</b>
Palm Oil Yield	0.0029*** (0.0004)	0.0032*** (0.0009)	0.0029*** (0.0004)	0.0035*** (0.0008)
Geographic	No	Yes	No	Yes
Yield potential	No	Yes	No	Yes
Socioeconomic	No	Yes	No	Yes
Observations	39,497	39,497	39,497	39,497

*Notes:* This table presents first-stage regression results predicting palm oil expansion. The instrument is the palm oil potential yield. Columns (1) and (2) present first-stage estimates based on logit models, while Columns (3) and (4) are estimated using scobit models. Coefficients marked with \*\*\* are significant at the 1% level. Standard errors, shown in parentheses, are clustered at the pixel level.